Polymer 51 (2010) 5165–5171

Contents lists available at ScienceDirect

Polymer

journal homepage: www.elsevier.com/locate/polymer

Influence of physical interaction between organoclay and poly(ethylene-co-vinyl acetate) matrix and effect of clay content on rheological melt state

V. Pistor*, A. Lizot, R. Fiorio, A.J. Zattera*

Laboratory of Polymers, Center of Exact Sciences and Technology (CCET), Caxias do Sul University (UCS), Caxias do Sul, RS, Brazil

ARTICLE INFO

Article history:
Received 16 June 2010
Received in revised form
16 August 2010
Accepted 21 August 2010
Available online 27 August 2010

Keywords:
EVA
OMMT
Nanocomposites

ABSTRACT

In this study nanocomposites of poly(ethylene-vinyl acetate) (EVA) and organophilic montmorillonite clay (OMMT) (0, 2, 5 and 10 phr) were prepared. The nanocomposites were characterized by X-ray diffraction (XRD), transmission electron microscopy (TEM), thermogravimetric analysis (TGA), parallel plate rheometry and mechanical analysis. Oscillatory rheometry provided relaxation and retardation spectra, and the stress relaxation modulus and the creep compliance curves were obtained using the nonlinear regularization (NLREG) program. The results showed that 2 phr of OMMT were not sufficient to promote dispersion and exfoliation of the clay, although in the form of clay tactoids it had a catalytic effect on the degradation of EVA. The OMMT content had a strong influence on the thermal stability of chain segments containing vinyl acetate (VAc). The rheological study showed that at 5 phr there were substantial changes in the viscosity and energy dissipation of the sample, suggesting that at above 2 phr the nanocomposites become more stable leading to changes in the creep and viscoelastic properties of the material. The addition of OMMT promoted significant gains in terms of the mechanical properties, and thus a study on the clay content and flow behavior was carried out.

1. Introduction

In the study of nanocomposites several researches have shown that these materials have different properties to thermoplastic materials, and also that the use of loads with nanometric dimensions leads to characteristics which differ from those obtained through reinforcement with microstructural loads [1]. Thus, in order to understand the nature of the dispersion and the specific properties obtained, several nanostructural composites have been tested [2–5].

The types of morphologies observed in nanocomposites tend toward tactoids, which are more likely than microcomposites, to promote the intercalation of the clay with the polymer matrix and exfoliation of the clay layers, thereby increasing their dispersion [6].

According to Marini et al. [7] the use of clays modified with polar surfactants leads to more efficient exfoliation with polar polymers under the best processing conditions. Of the several polar polymers available the thermoplastic composite poly(ethylene-vinyl acetate) (EVA) has been studied in relation to the incorporation of nanoclays [7–13]. EVA is a copolymer which has properties intermediate to those of its two constituent homopolymers, that is, polyethylene and poly(vinyl acetate) (PVAc). It properties are the result of its complex morphology, which is composed of a crystalline phase (containing ethylene units), an interfacial region (with ethylene and VAc segments) and a complex amorphous phase (with ethylene segments and non crystallized units of VAc) [14].

Zhang et al. [9] evaluated the effect of different types of clay in EVA matrices containing 28, 40, 50 and 80% (m/m) VAc. The authors observed that the clays containing modifying agents favored the passing of EVA chains between the clay platelets by increasing the basal spacing. They also noted that the polarity of the EVA is an important factor in terms of the morphology and properties of nanocomposites, and that EVA containing 28% (m/m) VAc showed more pronounced improvements in the thermal and mechanical properties.

Mantia and Dintcheva [11], studying the rheological behavior of the isothermal and non isothermal elongational flow of EVA/MMT nanocomposites processed in a twin-screw extruder, observed that with increasing charge there is a greater interlayer distance, increasing the loss and storage moduli as well as the viscosity in comparison to pure EVA.

Having established that the use of modified clays leads to more efficient exfoliation and dispersion of the nanoparticles, and thus can promote better dispersion and increased viscosity as well as greater rigidity, there is a need to understand the influence of the nanoclay content on the properties and processing of these materials.

Therefore, the aim of this study was to evaluate the influence of the addition of organophilic montmorillonite clay (OMMT) on the

* Corresponding authors. Tel.: +55 54 3218 2108; fax: +55 54 3218 2253.
E-mail addresses: vpistor1@ucs.br (V. Pistor), ajzatter@ucs.br (A.J. Zattera).

0032-3861/$ – see front matter © 2010 Elsevier Ltd. All rights reserved.
doi:10.1016/j.polymer.2010.08.045

morphological, thermal, mechanical and viscoelastic properties of poly(ethylene-vinyl acetate) (EVA)/OMMT nanocomposites. In assessing the viscoelastic properties, data from the relaxation and retardation spectra were used to obtain the stress relaxation modulus and the creep compliance curves through the nonlinear regularization (NLREG) program [15].

2. Materials

The materials used in this study were: poly(ethylene-co-vinyl acetate) (EVA); (UE-2824/32) containing 28% vinyl acetate (VAc), supplied by Polietilenos União S/A, and the nanoclay Cloisite 30B Montmorillonite $(CH_3)2N+$ (tallow) (CH_2CH_2OH), supplied by Southern Clay Products.

3. Methods

3.1. Characterization of nanocomposites

The EVA nanocomposites were processed by varying the concentration of montmorillonite clay (0, 2, 5 and 10 parts per hundred − phr). The mixtures were obtained after drying in a clay oven with air circulation at 60 °C for 8 h. Samples were prepared by the melt mixing process in a co-rotating interpenetrating twin-screw extruder (MH-COR-20-32-LAB, MH Equipamentos; $D = 20$ mm, $L/D = 32$). Eight heating zones and temperature profiles of 100, 120, 140, 160, 130*, 160, 160 and 160 °C, respectively, and a speed rotation of 400 rpm were used with the aid of vacuum degassing (zone 5*).

The X-ray diffractograms were collected on a sample holder mounted on the Shimadzu diffractometer (XRD-6000), with monochromatic Cu Kα radiation ($\lambda = 0.15418$ nm) and with the generator working at 40 kV and 30 mA. Intensities were measured in the range of $1^\circ < 2\theta < 12^\circ$, typically with scan steps of 0.05° and 2 s/step (1.5°min^{-1}).

For the transmission electron microscopy (TEM) the samples were prepared using cryo-ultramicrotomy. They were mounted on cryo-pins and frozen in liquid nitrogen. Analyses were performed in a JEOL transmission electron microscope (model JEM 1200 EX II) with a filter and operating at 80 kV.

The thermogravimetric analysis (TGA) was performed on a Shimadzu model TGA-50, with heating ramp of 10 °C min^{-1} under N_2 atmosphere (50 mL min^{-1}), using approximately 10 mg of sample.

The samples were analyzed in an Anton Paar oscillatory rheometer (Physica MCR 101), with parallel plates of 25 mm diameter and spacing between the plates of 1 mm, test temperature of 160 °C, frequency range of 0.1–100 Hz, test stress maximum of 200 Pa and nitrogen flow of 1 m^3/h. From the rheological analysis the relaxation ($H(\tau)$) and retardation ($L(\tau)$) spectra were collected, and the stress relaxation modulus ($G(t)$) and creep compliance ($J(t)$) curves were obtained using the nonlinear regularization (NLREG) program [15].

The Shore *D* hardness test was conducted with a Teclock Shore *D* durometer (GS 702), according to ASTM *D* 2240. The tensile strength tests were performed on type IV specimens (ASTM *D* 638), using an extensometer with a maximum deflection of 250 mm and a 200 kg.f load cell (EMIC DL 3000). Tear resistance tests (ASTM *D* 624) were performed in a universal testing machine (EMIC DL 3000) to measure the force required to tear the specimen at a specific speed of separation of 500 mm min^{-1}.

3.2. Viscoelastic model

The time dependence of relaxation phenomena is a complex factor, and measured modulus or compliance values will be strongly dependent on the exact manner in which the experiment is carried out.

It is known that through performing experiments at low strain amplitudes, the relaxation modulus can be obtained at all levels of deformation [16]. However, several physical functions, such as the relaxation spectra $H(\tau)$, cannot be calculated directly experimentally. However, these functions can be obtained from an experimentally measurable quantity by solving an inverse problem [17].

Through the use of Tikhonov regularization in its generalization for nonlinear inverse problems, called the nonlinear regularization (NLREG) method and implemented in the NLREG program, it becomes possible to obtain functions such as the spectrum of relaxation ($H(\tau)$), retardation ($L(\tau)$), stress relaxation modulus ($G(t)$) and creep compliance ($J(t)$) [15].

These viscoelastic functions can be obtained from the storage (G') and loss modulus (G'') from the following relations:

$$G'(\omega) = G_\theta + \int_{-\infty}^{\infty} H(\tau)\frac{\omega^2\tau^2}{1+\omega^2\tau^2}d\ln\tau \tag{1}$$

$$G''(\omega) = \int_{-\infty}^{\infty} H(\tau)\frac{\omega^2\tau^2}{1+\omega^2\tau^2}d\ln\tau \tag{2}$$

where: G_θ is the equilibrium modulus, $H(\tau)$ is a function of the relaxation spectrum, and τ is the relaxation time or deceleration.

The relaxation spectrum is the result of an infinite sum of Maxwell elements that describe the mechanical behavior of the elastic portion of the polymer and its ability to store energy [15,16,18] (Eq. (3)). Estimates of the retardation spectrum are obtained through the inter-relationships of the spectra described by Ferry and the results from the infinite sum of Voigt elements that are responsible for any portion of the viscous polymer [16] (Eq. (4)).

$$H(\tau) = \frac{L(\tau)}{\left[J_g + \int_{-\infty}^{\infty}\frac{L(\tau)}{(1-\tau)/\tau}d\ln\tau - \frac{\tau}{\eta_0}\right]^2 + \pi^2 L(\tau)^2} \tag{3}$$

$$L(\tau) = \frac{H(\tau)}{\left[G_\theta - \int_{-\infty}^{\infty}\frac{H(\tau)}{\tau/(\tau-1)}d\ln\tau\right]^2 + \pi^2 H(\tau)^2} \tag{4}$$

where: J_g is the instantaneous compliance, η_0 is the zero-shear viscosity and G_θ refers to the equilibrium modulus. Thus, the

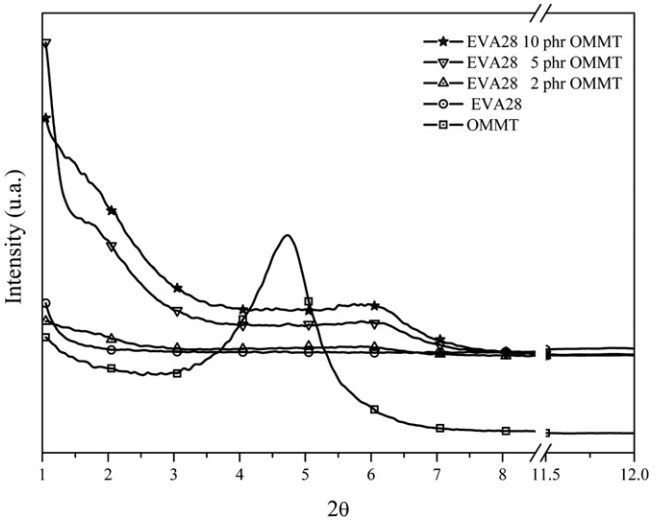

Fig. 1. XRD diffractograms obtained for the samples studied.

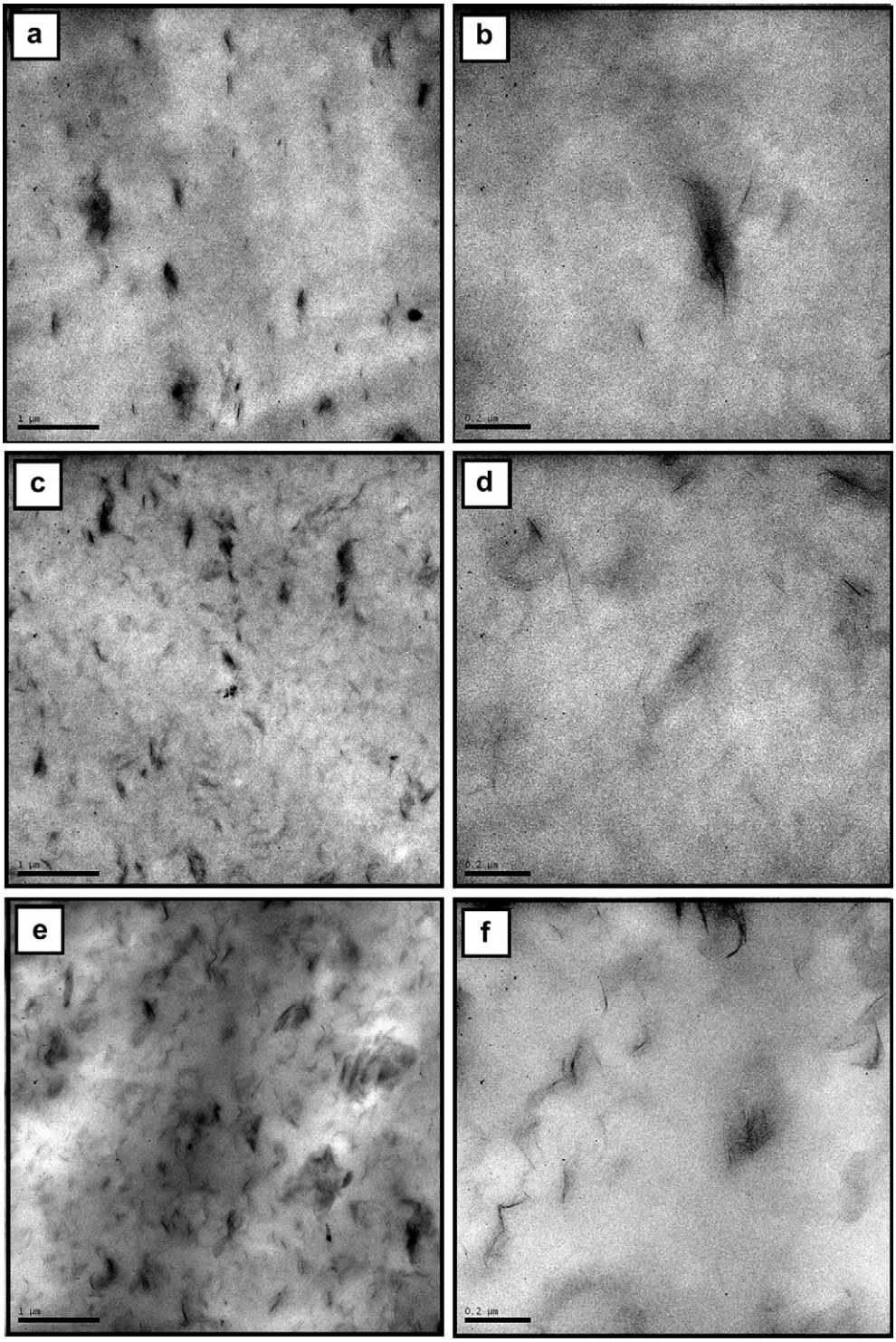

Fig. 2. Images of transmission electron microscopy (TEM) obtained for the nanocomposite where: (a; b) EVA 2 phr OMMT, (c; d) EVA 5 phr OMMT and (e; f) EVA 10 phr OMMT.

creep compliance function for viscoelastic liquids is approximately given by:

$$J(t) = J_g + \int_{-\infty}^{\infty} l(\tau)\left(1 - e^{-t/T}\right) d\ln\tau + \frac{t}{\eta^0} \quad (5)$$

Because the creep compliance ($J(t)$) function decays slowly over time, using an interface similar to the stress relaxation modulus ($G(t)$) requires that $J(t)$ relates to a decreasing function. Thus, $G(t)$ can be obtained from the following relationship:

$$G(t) = G_e + \int_{-\infty}^{\infty} \ln(\tau) e^{-t/\tau} d\ln\tau \quad (6)$$

4. Results and discussion

4.1. Dispersal and morphology of clay

The incorporation of the organophilic montmorillonite (OMMT) by mixing in the molten state in a twin-screw extruder was found

to be an appropriate method since the co-rotating screws and interpenetration promotes the efficient dispersion of the clay and exfoliate [6,11,19–21]. Fig. 1 shows the X-ray diffraction (XDR) pattern obtained for the nanocomposites containing 2, 5 and 10 parts per hundred (phr) of OMMT in the EVA matrix and also the diffractogram of the pure EVA and OMMT samples for comparison.

As can be seen the diffractogram for the OMMT 30B shows a diffraction peak at $2\theta \approx 4.8$ for the corresponding crystalline plane (001) [21,22]. Regarding the incorporation of OMMT, a relationship can be observed between the intensity and the addition of OMMT.

Marini et al. [7] studied the effect of viscosity on the exfoliation in nanocomposites of EVA/OMMT 30B and found that a lower diffraction peak (in this case the crystal plane (001) of the nanoclays) indicates a higher degree of exfoliation. The features of the nanocomposite morphologies with different clay contents can be observed in Fig. 2.

The incorporation of 2 phr led to a predominantly tactoid morphology (Fig. 2), possibly because this amount is insufficient for the dispersion and exfoliation. For the samples containing 5 and 10 phr of OMMT partial intercalation and exfoliation were the predominant characteristics observed and these samples also contained a small tactoid fraction.

According to Lee et al. [23], the absence of a diffraction peak and the dispersion characteristics observed in the TEM images are factors which confirm the nanocomposite structure. Moreover, these authors also describe that an increase in the vinyl acetate (VAc) content in the EVA matrix increases the exfoliation and dispersion of the clay due to the higher polarity and stronger interactions between the polymer and the clay.

4.2. Thermal stability

The results of the study on the thermal stability of the EVA and nanocomposite samples are shown in Fig. 3. Two distinct bands of degradation can be observed. The first mass loss, in the range of 270–370 °C, is related to the thermal decomposition of vinyl acetate $\{-CH_2-CH_2(O(-COCH_3)-)_m$ to form acetic acid and double bonds in the polymer backbone. The second mass loss, in the range of 380–500 °C, corresponds to degradation of the ethylene segments $(-CH_2-CH_2-)_n$ [24]. In the case of the first mass loss event the addition of OMMT promoted a shift in the acetate degradation to lower temperatures.

Riva et al. [8] studied the degradation of nanocomposites and observed a strong catalytic effect of the presence of various organoclays on the deacetylation of EVA containing 19% (m/m) vinyl acetate (VAc). More specifically, the authors found that the presence of the organic modifier has a catalytic effect on the production of H^+ at the active sites on the surface of silicates.

Costache et al. [10] studied the thermal decomposition of EVA nanocomposites (VAc28%)/OMMT30B. The authors incorporated 3 and 7% of clay and observed that loss of acetic acid is accelerated as a function of clay loading; the authors also attributed this acceleration to the catalytic effect of acid sites of the clay.

Therefore, on increasing the OMMT fraction, degradation of the acetate content occurs at a higher rate. This catalytic effect was noted even for 2 phr of nanoclay, indicating some interaction between the matrix and the dispersed phase. This is probably due to a more exfoliated morphology system, which generates higher contact area. Thus, by increasing the clay content (5 and 10 phr) greater interaction between the acetate groups and the terminal hydroxyl groups of the clay can occur.

The second degradation stage is related to the ethylene segments of EVA. The weight loss derivative (DTGA) shows that on increasing the OMMT content there is a tendency toward a reduction in the DTGA peak intensity. This reduction may be associated with the incorporation of clay. This hypothesis can be confirmed by the residual weight, which is proportional to the clay content.

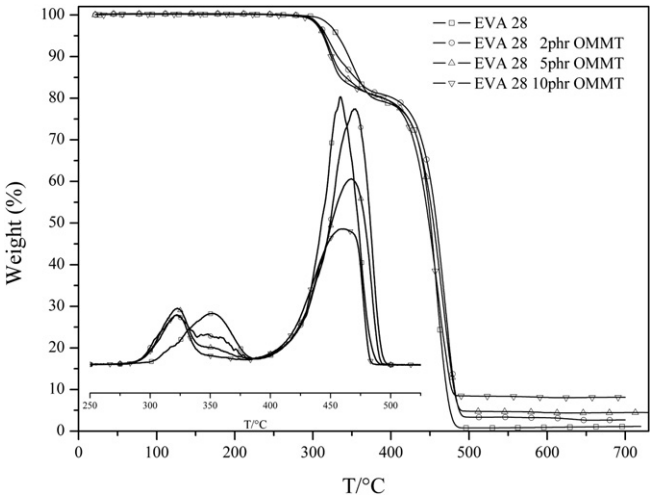

Fig. 3. Thermal degradation and differential thermal degradation (DTGA) curves obtained at a heating rate of 10 °C min^{-1} for EVA nanocomposites studied.

4.3. Viscoelastic properties

Fig. 4 shows the storage modulus (G′) and loss modulus (G″). In a dynamic experiment in the molten state at low frequencies, G″ is greater than G′ at high frequencies and G′ tends to increase at a greater rate than G″, as in the molten state power dissipation is dependent on the time required for the chains to respond to a sinusoidal stress at a certain applied force [21].

These characteristics show that an increase in OMMT content promoted an increase in the modulus values. But with increasing levels of OMMT at low frequencies G′ and G″ tend to be closer. This phenomenon can be observed through the ratio between the loss and storage moduli in Fig. 5, which is called the loss factor or loss tangent (tan δ) Eq. (7) [16].

$$\tan\delta = G''/G' \tag{7}$$

For the dimensional stability of the system under study, it is considered that the closer the ratio of the moduli is to unity, the

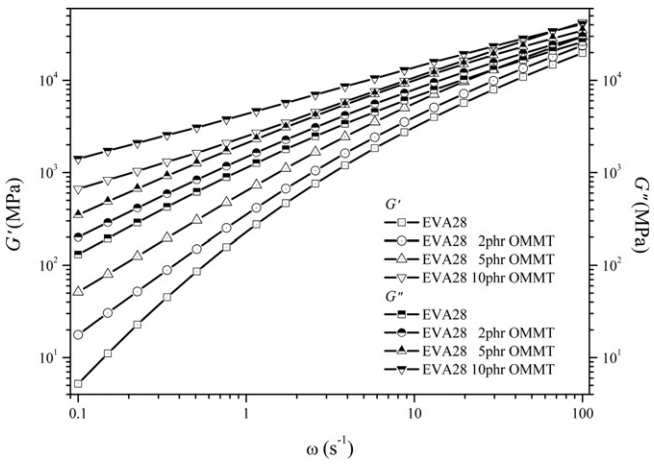

Fig. 4. Storage (G′) and loss (G″) moduli obtained from the samples studied by oscillatory rheometry.

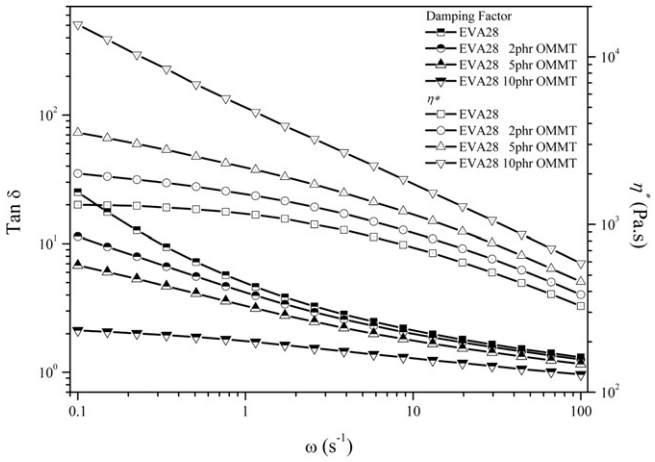

Fig. 5. Tan δ curves and complex viscosity (η^*) obtained from the samples studied by oscillatory rheometry.

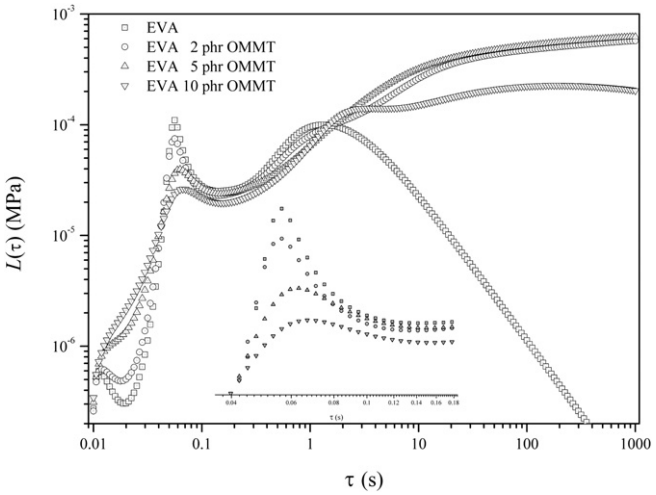

Fig. 7. Retardation spectra obtained for the samples studied.

lower the energy loss in relation to its storage capacity, *i.e.* the lower dissipation of energy in the system promotes greater difficulty in the handling of the polymer chains [21]. Hyun et al. [25] carried out rheological measurement of the nanocomposites and reported that the dispersion level of particles can be considered as non associated, weakly associated and strongly associated for ($\tan\delta > 3$) ($1 < \tan\delta < 3$) and ($\tan\delta < 1$), respectively. In Fig. 5, it was observed that at frequencies of up to 1 s^{-1}, only the sample containing 10 phr of OMMT showed a strongly associated particle dispersion [25].

Moreover, for the dimensional stability of the system under study, it is considered that the closer the ratio of the moduli is to unity, the lower the energy loss in relation to its storage capacity, *i.e.* the lower dissipation of energy in the system promotes greater difficulty in the handling of the polymer chains [21]. This reflected in an increase in the complex viscosity (η^*) observed in Fig. 5. The increase in complex viscosity with respect to increasing levels of OMMT may also be associated with good dispersion of the clay in the matrix, with the strong interaction of the acetate groups with OH end groups in the clay 30B [9,23].

The VAc content in the EVA is a crucial factor in terms of the structure of EVA/clay nanocomposites; Zhang et al. [9] observed that an increase in VAc content increased both the polarity and flexibility of EVA chains by promoting the passage of chains between the galleries of the clay, leading to the formation of intercalated structures.

La Mantia and Tzankova Dintcheva [11] reported that an increase in viscosity in the presence of nanoclays dispersed in a twin-screw extruder, reflects the non-Newtonian behavior becoming more pronounced, probably due to good dispersion and a greater strain-hardening effect in the isothermal elongational flow compared to pure EVA.

Pavlidou and Papaspyrides [6] described that more exfoliated clay can lead to better interaction due to factors such as increased surface contact area, percolation of the clay dispersed in the matrix and a larger volume of nanoparticles dispersed per unit area. These relationships corroborate Fig. 2, where on increasing the OMMT content a greater distribution of the dispersed clay per unit area can be observed, along with greater exfoliation of the clay also generating a larger contact area.

Marini et al. [7] emphasize that good interaction with the organoclay EVA observed in terms of increased viscosity is due to the pseudo-solid behavior through exfoliation and good dispersion of clay providing more stability in the molten state in relation to the matrix.

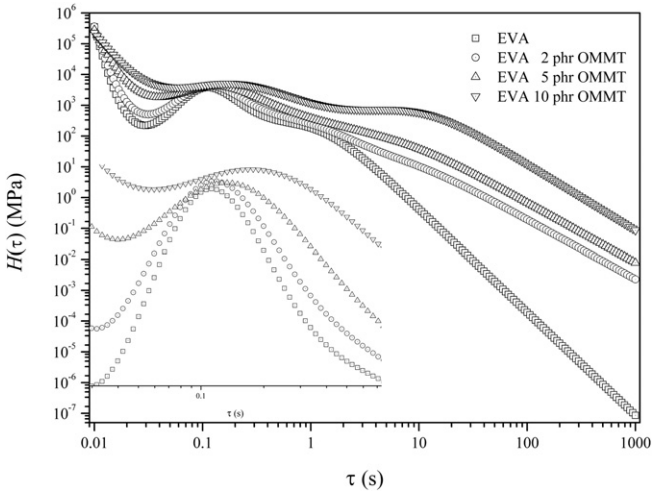

Fig. 6. Relaxation spectra obtained for the samples studied.

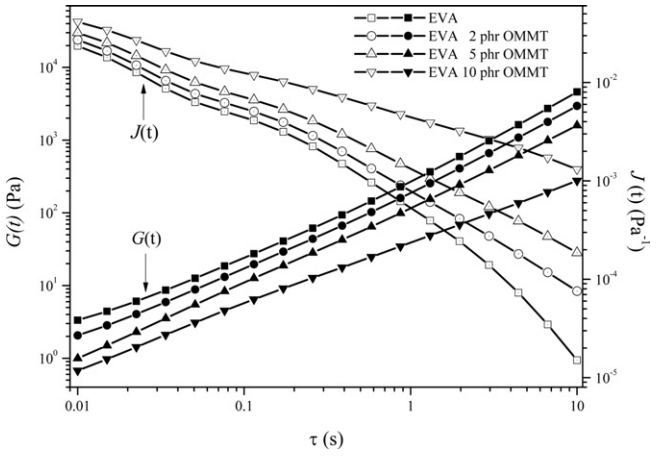

Fig. 8. Stress relaxation modulus ($G(t)$) (solid symbols) and creep compliance ($J(t)$) (open symbols) obtained for the samples studied.

Fig. 6 shows the relaxation spectra ($H(\tau)$) obtained. Regarding the EVA, two characteristic relaxation peaks can be seen at 0.1 and 1 s.

The initial relaxation phenomenon of $\tau \approx 0.1$ s is possibly related to the molecular weight distribution and changes in the conformation, where the smaller molecules tend to relax first and the degree of freedom derived from the chains in the melt enables conformational rearrangement of the chain segments [26].

The second phenomenon of relaxation ($\tau \approx 1$ s) can be related to the type and amount of branching as the spatial hindrance imposed by large segments of the branches provided by the ethylene would logically result in a delay in the relaxation in relation to smaller chains.

As a result of the distribution of relaxation times and the strong dependence on the size and type of chains involved these phenomena tend to be extended across cooperative relaxation effects [16], and the relaxation can propagate along the chains, involving an increasing number of main chain segments over time [26]. With the addition of OMMT, it was possible to observe peak broadening in the relaxation ($\tau \approx 0.1$ s) and a shift of the second peak from $\tau \approx 1$ s to $\tau \approx 10$ s with the increase in OMMT content. The longest relaxation times and the best distribution are related to the elastic component of the system [15,16,18], *i.e.* with the addition of OMMT it appears that the system becomes structurally stronger, thereby increasing the ability to store energy and enabling the cooperative effects of more prolonged relaxation and retardation over time.

Corroborating these results, Fig. 7 shows the retardation spectra related to the viscous component of the system [16]. A reduction in the retardation peak at approximately ($\tau \approx 0.06$ s) can be observed and this is analogous to the relaxation phenomena discussed earlier.

It was also shown that on increasing the OMMT content the distribution of retardation times tends to be lower due to the reduction in the viscous component. This behavior confirms the results for tan δ observed in Fig. 5, where it was found that with the addition of OMMT the ratio of the moduli tends to unity, demonstrating that the system has become structurally stronger than pure EVA.

Considering again the study by Marini et al. [7], the authors also showed longer relaxation times for OMMT nanocomposites (Cloisite 30B) and associated this with the behavior of a pseudo-solid sample.

Thus, considering this behavior, Fig. 8 illustrates the curves for the stress relaxation modulus ($G(t)$) and creep compliance ($J(t)$) to better understand the relationship between dimensional stability and creep in the systems studied. It can be seen that the increase in OMMT content promoted a significant increase in $G(t)$, corroborating the relaxation times shown.

Dal Castel et al. [18] studied viscoelastic functions obtained through the program NLREG for nanocomposites of polypropylene (PP)/MMT using EVA and poly (ethylene-co-vinyl alcohol) (EVOH) as compatibilizers and observed an increase in $G(t)$ for the composition containing 92, 5, 3 w.% of PP, EVA and MMT, respectively. The authors describe this behavior as a result of the increase in structural rigidity caused by the presence of MMT and attributed this phenomenon to the formation of a physical network between the platelets which can act as a mechanism of energy dissipation.

These characteristics could be consideration in the case of the EVA/OMMT nanocomposites, however, the observed increase in $G(t)$ with increasing levels of OMMT may also be associated with the strong interaction between the VAc and terminal hydroxyl groups of the clay [8,10] further contributing to the formation of a physical network which is more rigid due to interpenetration of the polymer chains in the structure of the exfoliated and intercalated clay.

The $J(t)$ curves in Fig. 8 show that the contribution of the presence and increasing content of OMMT to a restriction in the flow of material is proportional to the increase in η^* (Fig. 5) and is consistent with the increase in relaxation times observed in Fig. 6 and also the increase in $G(t)$.

The Fig. 9 shows a hypothetical segment chain to better understand the effect of OMMT in the EVA matrix. Assuming that in a dynamic test in the melt state with a sinusoidal frequency of 1–100 Hz at a temperature of 160 °C and at a maximum stress of 200 Pa is able to orient and relax the hypothetical chain segment in the direction of force applied, then the presence of exfoliated clay in the EVA matrix can be better understood through the free volume of polymer chains in the melt state.

In the melt state the free volume is large, molecular movements occur easily, and the degrees of freedom facilitate the mobility of molecules which are thus able to freely change their conformation enabling molecular relaxation [16,26].

It can be concluded from the rheological phenomena observed with the addition of OMMT that the dispersion of clay impedes the mobility and conformation of the polymer chains reducing the possibility of conformation of the chains occurring. Since the dispersion of clay was effective and the exfoliated and partially exfoliated structures can lead to a reduction in the degrees of

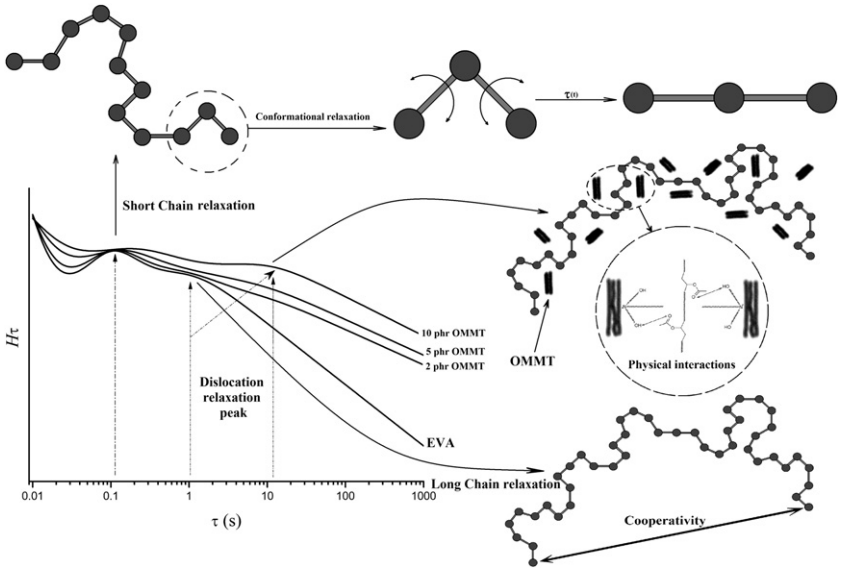

Fig. 9. Proposed scheme for understanding the relaxation phenomena related to the addition of OMMT.

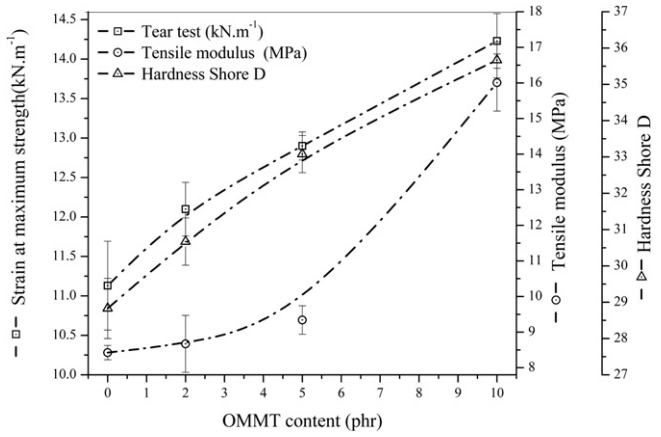

Fig. 10. Results from mechanical tests for the nanocomposites studied.

freedom and greater interaction between the load/polymer, the effect of relaxation through cooperativity establishes the existence of a network of interactions along the polymer matrix.

This hypothesis is evidenced by the shift in the relaxation time from $\tau \approx 1$ s to $\tau \approx 10$ s with the increase in OMMT content, and also the flow restriction and increased rigidity of the system are seen through the $J(t)$ and $G(t)$ curves, respectively.

4.4. Mechanical properties

The mechanical properties shown in Fig. 10 were obtained in order to compare the viscoelastic properties of the melt with the gains from the addition of OMMT in a possible final application. As can be seen, in terms of the mechanical properties, adding up to 10 phr promoted an increase of ≈54% in the tear strength, ≈88% in the tensile modulus and ≈22% in the hardness (Shore *D*) compared to the properties of EVA (28% VAc).

Both the higher values for tear resistance and the greater rigidity observed through the increased value for the tensile modulus, as well as the greater resistance to penetration evidenced by the behavior of the hardness (Shore *D*), are directly related to the strong interaction between the matrix and nanoclay used. The increased stability of the system is a reflection of the good characteristics and good dispersion of exfoliated clay. However, a restricted flow was observed through the behavior of both the viscosity and the creep compliance curves. This is a strong indication that the amount of clay and the processing conditions for product manufacture should be taken into consideration since the system becomes structurally stronger even in the molten state, where the free flow is directly related to the ability of the material to flow and take the direction of flow required for the processing of the polymeric material.

5. Conclusions

EVA nanocomposites with different contents of montmorillonite clay were studied. The results of the X-ray diffraction and transmission electron microscopy confirmed the exfoliation and dispersion of the clay. However, it was shown that in terms of exfoliation the incorporation of 2 phr of clay was not effective, since exfoliation did not occur and therefore the clay could not be dispersed in the EVA matrix.

The thermal degradation results showed that even in the form of tactoids the sample containing 2 phr of clay undergoes catalytic degradation in the VAc degradation temperature range, due to the interaction between the organoclay and the EVA matrix. We also observed a strong relationship between clay content and the VAc degradation rate, and the residual mass of each sample corresponded to the levels incorporated in the extrusion process, showing that the samples were dispersed homogeneously throughout the matrix EVA.

It was found through oscillatory rheometry that the increase in the clay content led to an increased capacity to store energy, and this capacity led to a greater stability of the material which in turn dissipates less energy. Both the increase in viscosity and the tan δ curves showed a considerable increase in the stability of the melting polymer.

Thus, through the relaxation and retardation spectra it was possible to understand that both the increase in viscosity and the lower energy dissipation show that the presence of nanoclays changes the relaxation behavior under stress in the melting state. The increase in relaxation times with increasing clay content was corroborated by high modulus values for relaxation under tension and reduced material flow.

The increased stability of the nanocomposites above 2 phr in the melt state showed that the exfoliated nanoclay in addition to generating restrictions in the free volume also has strong physical interactions with the EVA matrix, restricting the degrees of freedom of the chains and reducing the material flow. This strong interaction results in significant gains in terms of the mechanical properties, as illustrated in this study. However, it was observed that the flow behavior in a dynamic test undergoes significant changes and it should be considered that the addition of clay at different levels requires the optimization of the processing conditions in relation to those used for the pure EVA matrix.

Acknowledgements

The authors of this study gratefully acknowledge the UCS, CNPq, FAPERGS by granting scholarships and financial aid received.

References

[1] Paul DR, Robeson LM. Polymer 2008;49:3187–204.
[2] Cassagnau Ph. Polymer 2008;49:2183–96.
[3] Pfaendner R. Polym Degrad Stab 2010;95:369–73.
[4] Madaleno L, Schjødt-Thomsen J, Pinto JC. Compos Sci Technol 2010;70:804–14.
[5] Schlemmer D, Angélica RS, Sales MJA. Compos Struct 2010;92:2066–70.
[6] Pavlidou S, Papaspyrides CD. Prog Polym Sci 2008;33:1119–98.
[7] Marini J, Branciforti MC, Lotti C. Polym Adv Technol 2009, doi:10.1002/pat.1444.
[8] Riva A, Zanetti M, Braglia M, Camino G, Falqui L. Polym Degrad Stab 2002;77:299–304.
[9] Zhang W, Chen D, Zhao Q, Fang Y. Polymer 2003;44:7953–61.
[10] Costache MC, Jiang DD, Wilkie CA. Polymer 2005;46:6947–58.
[11] La Mantia FP, Dintcheva NT. Polym Test 2006;25:701–8.
[12] Mishra SB, Luyt ASJ. Appl Polym Sci 2009;112:218–25.
[13] Sureshkumar MS, Filippi S, Polacco G, Kazatchkov I, Stastna J, Zanzotto L. Eur Polym J 2010;46:621–33.
[14] Yamaki SB, Prado EA, Atvars TDZ. Eur Polym J 2002;38:1811–26.
[15] Roths T, Marth M, Weese J, Honerkamp J. Comput Phys Commun 2001;139:279–96.
[16] Ferry JD. Viscoelastic properties of polymers. 3rd ed. New York: John Wiley & Sons; 1980.
[17] Weese J. Comput Phys Commun 1993;77:429–35.
[18] Dal Castel C, Bianchi O, Oviedo MAS, Liberman SA, Mauler RS, Oliveira RVB. Mat Sci Eng C 2009;29:602–6.
[19] Pasanovic-Zujo V, Gupta RK, Bhattacharya SN. Rheol Acta 2004;43:99–108.
[20] Gupta RK, Pasanovic-Zujo V, Bhattacharya SNJ. Non-Newtonian Fluid Mech 2005;128:116–25.
[21] Hong-mei Y, Qiang Z, Miao D. Chem Res Chin Univ 2006;22:651–7.
[22] Chaudhary DS, Prasad R, Gupta RK, Bhattacharya SN. Thermochim Acta 2005;433:187–95.
[23] Lee HM, Park BJ, Jin Choi H, Gupta RK, Bhattachary SNJ. Macromol Sci, Part B: Phys 2007;46:261–2737.
[24] Rodríguez-Vázquez M, Liauw CM, Allen NS, Edge M, Fontan E. Polym Degrad Stab 2006;91:154–64.
[25] Hyun YH, Lim ST, Choi HJ, Jhon MS. Macromolecules 2001;34:8084–93.
[26] Matsuoka S. Relaxation phenomena in polymers. Munich: Hanser Publishers; 1992.